Decay Rates in Attractive Bose-Einstein Condensates

C. Huepe,[1] S. Métens,[1] G. Dewel,[2] P. Borckmans,[2] and M. E. Brachet[1]
[1]*Laboratoire de Physique Statistique de l'Ecole Normale Supérieure, associé au CNRS et aux Universités Paris 6 et 7, 24 Rue Lhomond, 75231 Paris Cedex 05, France*
[2]*Service de Chimie-Physique and Center for Nonlinear Phenomena and Complex Systems, CP 231, Université Libre de Bruxelles, 1050 Bruxelles, Belgium*
(Received 17 August 1998)

Attractive Bose-Einstein condensates are investigated with numerical continuation methods capturing stationary solutions of the Gross-Pitaevskii equation. The branches of stable (elliptic) and unstable (hyperbolic) solutions are found to meet at a critical particle number through a generic Hamiltonian saddle node bifurcation. The condensate decay rates corresponding to macroscopic quantum tunneling, two and three body inelastic collisions, and thermally induced collapse are computed from the exact numerical solutions. These rates show experimentally significant differences with previously published rates. Universal scaling laws stemming from the bifurcation are derived. [S0031-9007(99)08550-6]

PACS numbers: 03.75.Fi, 05.30.Jp, 32.80.Pj, 47.20.Ky

Experimental Bose-Einstein condensation (BEC) in ultracold vapors of ^{7}Li atoms [1] opened a new field in the study of macroscopic quantum phenomena. Condensates with attractive interactions are known to be metastable in spatially localized systems, provided that the number of condensed particles is below a critical value $\mathcal{N}_c$ [2]. Various physical processes compete to determine the lifetime of attractive condensates. Among them one can distinguish macroscopic quantum tunneling (MQT) [3,4], inelastic two and three body collisions (ICO) [5–7], and thermally induced collapse (TIC) [4,8]. The MQT and TIC contributions were evaluated in the literature using a variational Gaussian approximation to the condensate density. However, this approximation is known to be in substantial quantitative error—e.g., as high as 17% on $\mathcal{N}_c$ [3,9]—when compared to the exact solution of the Gross-Pitaevskii (GP) equation. Experimentally, the recent observations of Feshbach resonances in BEC of sodium atoms offer new possibilities to investigate the dynamics of condensates with negative scattering lengths close to zero temperature (in the nK range) [10]. Reliable theoretical evaluations of the lifetime of metastable condensates are thus needed for quantitative comparisons with experiments.

The basic goal of the present Letter is to numerically compute the bifurcation diagram of the stationary solutions of the GP equation. Both the stable (elliptic) and unstable (hyperbolic) branches of solutions will then be used to obtain decay rates and compare them to the known (Gaussian approximation) ones. At low enough temperature, neglecting the thermal and quantum fluctuations, a Bose condensate can be represented by a complex wave function $\psi(\mathbf{x}, t)$ that obeys the dynamics of the GP equation [11,12]. Specifically, we consider a condensate of $\mathcal{N}$ particles of mass m and (negative) effective scattering length a in a radial confining harmonic potential $V(r) = m\omega^2 r^2/2$. Using variables rescaled by the natural quantum harmonic oscillator units of time $\tau_0 = 1/\omega$ and length $L_0 = \sqrt{\hbar/m\omega}$: $\tilde{t} = t/\tau_0$, $\tilde{\mathbf{x}} = \mathbf{x}/L_0$, and $\tilde{a} = 4\pi a/L_0$, the condensate is described by the action

$$\mathcal{A} = \int d\tilde{t}\left\{\int d^3\tilde{\mathbf{x}}\,\frac{i}{2}\left(\bar{\psi}\,\frac{\partial\psi}{\partial\tilde{t}} - \psi\,\frac{\partial\bar{\psi}}{\partial\tilde{t}}\right) - \mathcal{F}\right\}, \quad (1)$$

with $\mathcal{F} = \mathcal{E} - \mu\mathcal{N}$, where $\mathcal{N} = \int d^3\tilde{\mathbf{x}}|\psi|^2$ and

$$\mathcal{E} = \int d^3\tilde{\mathbf{x}}\left(\frac{1}{2}\,|\nabla_{\tilde{\mathbf{x}}}\psi|^2 + \frac{1}{2}\,|\tilde{\mathbf{x}}|^2|\psi|^2 + \frac{\tilde{a}}{2}\,|\psi|^4\right). \quad (2)$$

The Euler-Lagrange equation corresponding to $\mathcal{A}$ is our working form of the Gross-Pitaevskii equation:

$$-i\,\frac{\partial\psi}{\partial\tilde{t}} = -\frac{\delta\mathcal{F}}{\delta\bar{\psi}} = \frac{1}{2}\,\nabla^2_{\tilde{\mathbf{x}}}\psi - \frac{1}{2}\,|\tilde{\mathbf{x}}|^2\psi - (\tilde{a}|\psi|^2 - \mu)\psi\,. \quad (3)$$

We use the following experimental data corresponding to ^{7}Li atoms in a radial trap: $m = 1.16 \times 10^{-26}$ kg, $a = -23.3a_0$ (with a_0 the Bohr radius), and $\omega = (\omega_x\omega_y\omega_z)^{1/3} = 908.41\ \mathrm{s}^{-1}$. These values yield $\tilde{a} = -5.74 \times 10^{-3}$. With these parameters (3) is a mean-field approximation expected to be very reliable. Note that we ignore the contributions of noncondensed atoms. They interact with the condensate only through a nearly constant background density term, inducing no significant change in the dynamics of the system [13].

Stationary states of (3) corresponding to minima of $\mathcal{E}$ at a given value of $\mathcal{N}$ are obtained by integrating to relaxation the diffusion equation

$$\frac{\partial\psi}{\partial\tilde{t}} = -\frac{\delta\mathcal{F}}{\delta\bar{\psi}} = \frac{1}{2}\,\nabla^2_{\tilde{\mathbf{x}}}\psi - \frac{1}{2}\,|\tilde{\mathbf{x}}|^2\psi - (\tilde{a}|\psi|^2 - \mu)\psi\,, \quad (4)$$

where the Lagrange multiplier μ is fixed by the condition $\partial\mathcal{N}/\partial\tilde{t} = 0$. Note that dynamical solutions of (3) are only affected by μ through a homogeneous rotating phase

 0031-9007/99/82(8)/1616(4)$15.00

factor $e^{i\mu\tilde{t}}$. Pseudospectral methods [14] are used to solve (4). The radially symmetric $\psi(r,\tilde{t})$ is expanded as $\psi(r,\tilde{t}) = \sum_{n=0}^{N_R/2} \hat{\psi}_{2n}(\tilde{t}) T_{2n}(r/R)$, where T_n is the nth order Chebyshev polynomial and $\hat{\psi}_{N_R}$ is fixed to satisfy the boundary condition $\psi(R,\tilde{t}) = 0$. The results reported below were generated with $R = 4$ and $N_R = 256$. To integrate (4) we use the time stepping scheme

$$\psi(\tilde{t} + \sigma) = \Theta^{-1}\{\psi(\tilde{t}) - \sigma[r^2\psi/2 + (\tilde{a}|\psi|^2 - \mu)\psi]\}, \tag{5}$$

where $\Theta = 1 - \sigma\nabla^2/2$. This relaxation method is equivalent to that used in [9] and can only reach the stable stationary solutions of (4).

In order to numerically compute the full bifurcation diagram of (4) we also capture the previously unknown unstable stationary solutions using Newton branch following [15,16]. We start from a stable state obtained by relaxing (4) at a small value of $\mathcal{N}$. We search for fixed points of (5), a condition strictly equivalent to the stationarity of (3). Calling $\psi_{(j)}$ the value of the field ψ over the jth collocation point, we look for ψ^* such that $f_{(j)}(\psi^*) \equiv \psi^*_{(j)}(\tilde{t} + \sigma) - \psi^*_{(j)}(\tilde{t}) = 0$. At every Newton step we numerically solve $\sum_k [df_{(j)}/d\psi_{(k)}]\delta\psi_{(k)} = -f_{(j)}(\psi)$, for $\delta\psi_{(k)}$ [17], where σ controls the preconditioning of the Newton step [18]. Once the converged stationary solutions of (3) are obtained, $-i\delta\mathcal{F}/\delta\psi$ is linearized around them. The eigenvalues λ_n of the corresponding linear operator are computed by constructing and diagonalizing the associated matrix [16]. When the smallest absolute value λ is purely imaginary, $|\lambda|$ is the (adimensionalized) energy of small excitations.

The values of the energy functional $\mathcal{E}$ and the (smallest absolute value) square eigenvalue λ^2 versus particle number $\mathcal{N}$ are shown as solid lines in Fig. 1 (top and bottom, respectively). The eigenvalues are imaginary on the metastable elliptic lower branch ($\lambda^2 < 0$) and real on the unstable hyperbolic upper branch ($\lambda^2 > 0$). Using (1) on stationary solutions we obtain $d\mathcal{E}/d\mathcal{N} = \mu$. Thus μ is the slope of $\mathcal{E}$ and the lower branches $\mathcal{E}_-$, λ^2_- (respectively, upper branches $\mathcal{E}_+$, λ^2_+) are scanned for $\mu > \mu_c$ (respectively, $\mu < \mu_c$). The point $\mu = \mu_c$ determines the maximum number of particles $\mathcal{N} = \mathcal{N}_c$ for which stationary solutions exist. We have checked that all the other pairs of eigenvalues are imaginary on both branches (data not shown).

This qualitative behavior is the generic signature of a Hamiltonian saddle node (HSN) bifurcation defined, at lowest order, by the normal form [19]

$$m_{\text{eff}}\ddot{Q} = \delta - \beta Q^2, \tag{6}$$

where $\delta = 1 - \mathcal{N}/\mathcal{N}_c$ is the bifurcation parameter. The critical amplitude Q is related to the radius of the condensate [16] and the parameters β and m_{eff} can be linked to critical scaling laws. Indeed, defining the appropriate energy $\mathcal{E} = \mathcal{E}_0 + m_{\text{eff}}\dot{Q}^2/2 - \delta Q + \beta Q^3/3 - \gamma\delta$, it is straightforward to derive from (6), close to the critical point $\delta = 0$, the universal scaling laws

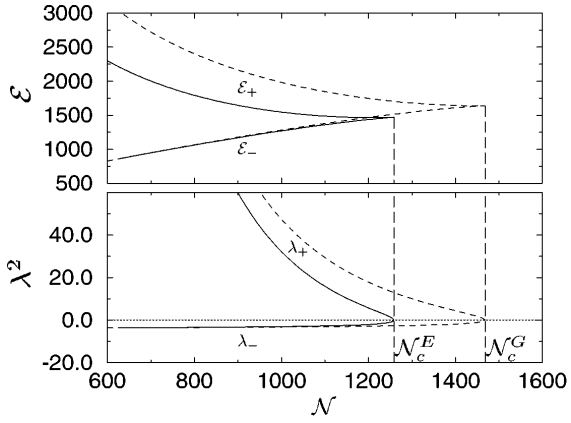

FIG. 1. Stationary solutions of the GP equation versus particle number $\mathcal{N}$. Top: value of the energy functional $\mathcal{E}_+$ on the stable (elliptic) branch and $\mathcal{E}_-$ on the unstable (hyperbolic) branch. Bottom: square of the bifurcating eigenvalue ($\lambda^2_\pm$); $|\lambda_-|$ is the energy of small excitations around the stable branch. Solid lines: exact solution of the GP equation. Dashed lines: Gaussian approximation.

$$\mathcal{E}_\pm = \mathcal{E}_c - \mathcal{E}_l\delta \pm \mathcal{E}_\Delta\delta^{3/2}, \tag{7}$$

$$\lambda^2_\pm = \pm\lambda^2_\Delta\delta^{1/2}, \tag{8}$$

where $\mathcal{E}_c = \mathcal{E}_0$, $\mathcal{E}_l = \gamma$, $\mathcal{E}_\Delta = 2/3\sqrt{\beta}$, and $\lambda^2_\Delta = 2\sqrt{\beta}/m_{\text{eff}}$. The dynamical content of the HSN normal form (6) can be understood by the following considerations. The phase space is separated in two regions by a separatrix (homoclinic orbit) that starts and ends at the hyperbolic fixed point. Trajectories inside the separatrix remain bounded near the elliptic fixed point. If the condensate is taken beyond the separatrix by a perturbation (e.g., thermal excitations or quantum tunneling, see below), it will fall into unbounded (hyperbolic) trajectories and collapse. As $\mathcal{N}$ approaches $\mathcal{N}_c$, the bounded region around the elliptic fixed point is reduced and the condensate becomes more unstable. At $\mathcal{N} = \mathcal{N}_c$ the elliptic fixed point meets the hyperbolic fixed point and the separatrix disappears. No stationary condensate can be formed for $\mathcal{N} > \mathcal{N}_c$.

The results obtained with the Gaussian approximation for the condensate density [20,21] are also shown in Fig. 1 as dashed lines. These approximate results can be obtained analytically by the following procedure: Inserting $\psi(r,\tilde{t}) = A(\tilde{t})\exp[-r^2/2r_G^2(\tilde{t}) + ib(\tilde{t})r^2]$ inside the action (1) yields a set of Euler-Lagrange equations for $r_G(\tilde{t})$, $b(\tilde{t})$, and the (complex) amplitude $A(\tilde{t})$. The stationary solutions of the Euler-Lagrange equations produce the following values [16]:

$$\mathcal{N}(\mu) = \frac{4\sqrt{2\pi^3}(-8\mu + 3\sqrt{7 + 4\mu^2})}{7|\tilde{a}|(-2\mu + \sqrt{7 + 4\mu^2})^{3/2}}, \tag{9}$$

$$\mathcal{E} = \mathcal{N}(\mu)(-\mu + 3\sqrt{7 + 4\mu^2})/7. \tag{10}$$

$\mathcal{N}$ is maximal at $\mathcal{N}_c^G = 8\sqrt{2\pi^3}/|5^{5/4}\tilde{a}|$ for $\mu = \mu_c^G = 1/2\sqrt{5}$. Linearizing the Euler-Lagrange equations around the stationary solutions, we obtain the eigenvalues [16]

$$\lambda^2(\mu) = 8\mu^2 - 4\mu\sqrt{7 + 4\mu^2} + 2. \quad (11)$$

As apparent in Fig. 1, the exact critical $\mathcal{N}_c^E = 1258.5$ is smaller than the Gaussian one $\mathcal{N}_c^G = 1467.7$ [3,9]. The critical amplitudes corresponding to the Gaussian approximation can be computed from (9) and (10). One finds $\mathcal{E}_c = 4\sqrt{2\pi^3}/|5^{3/4}\tilde{a}|$, $\mathcal{E}_\Delta = 64\sqrt{\pi^3}/|5^{9/4}\tilde{a}|$, and $\lambda_\Delta^2 = 4\sqrt{10}$. For the exact solutions, we obtain the critical amplitudes by performing fits on the data. One finds $\mathcal{E}_\Delta = 1340$ and $\lambda_\Delta^2 = 14.68$. Thus, the Gaussian approximation captures the bifurcation qualitatively but with quantitative 17% error on N_c [9], 24% error on $\mathcal{E}_\Delta$, and 14% error on λ_Δ^2. Figure 2 shows the physical origin of the quantitative errors in the Gaussian approximation. By inspection it is apparent that the exact solution is well approximated by a Gaussian only for small $\mathcal{N}$ on the stable (elliptic) branch.

The TIC decay rate Γ_T is estimated using the formula [22]

$$\Gamma_T/\omega = |\lambda_+/2\pi| \exp[-\hbar\omega(\mathcal{E}_+ - \mathcal{E}_-)/k_B T], \quad (12)$$

where $\hbar\omega(\mathcal{E}_+ - \mathcal{E}_-)$ is the (dimensionalized) height of the nucleation energy barrier, T is the temperature of the condensate, and k_B is the Boltzmann constant. Note that the prefactor characterizes the typical decay time which is controlled by the slowest part of the nucleation dynamics: the top-of-the-barrier saddle point eigenvalue λ_+ and not λ_- as used in [4]. However, near the bifurcation both eigenvalues scale in the same way and the behavior of Γ_T can be obtained directly from the universal saddle node scaling laws (7) and (8). Thus the exponential factor and the prefactor vanish, respectively, as $\delta^{3/2}$ and $\delta^{1/4}$.

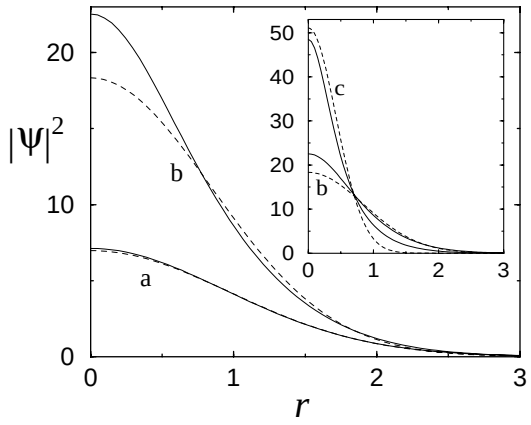

FIG. 2. Condensate density $|\psi|^2$ versus radius r, in reduced units (see text). Solid lines: exact solution of the GP equation. Dashed lines: Gaussian approximation. Stable (elliptic) solutions are shown for particle number $\mathcal{N} = 252$ (a) and $\mathcal{N} = 1132$ (b). (c) is the unstable (hyperbolic) solution for $\mathcal{N} = 1132$ (see inset).

We estimate the MQT decay rate using an instanton technique that takes into account the semiclassical trajectory giving the dominant contribution to the quantum action path integral [3,4]. We approximate this so-called bounce trajectory by the solution of the equation of motion $d^2q(t)/dt^2 = -dV(q)/dq$ starting and ending at the fixed point q_f of the phase space where $\mathcal{E}(q_f) = \mathcal{E}_-$. $V(q)$ is a polynomial such that $-V(q)$ reconstructs the Hamiltonian dynamics. Fixing $q = 0$ at the top, $\mathcal{E}_+$ point, the reconstruction condition implies the relations $V(0) = -\mathcal{E}_+$, $V(q_f) = -\mathcal{E}_-$, $\partial_q^2 V(0) = |\lambda_+(\mathcal{N})|$, and $\partial_q^2 V(q_f) = -|\lambda_-(\mathcal{N})|$ that uniquely determines $V(q) = \alpha_0 + \alpha_2 q^2 + \alpha_3 q^3 + \alpha_4 q^4$. We thus obtain a semianalytical polynomial expression with coefficients determined from the values presented in Fig. 1. Once $V(q)$ and the bounce point q_b [$V(q_b) = V(q_f)$] are known, the MQT rate is estimated as

$$\frac{\Gamma_Q}{\omega} = \sqrt{\frac{|\lambda_-|v_0^2}{4\pi}} \exp\left[\frac{-4}{\sqrt{2}} \int_{q_f}^{q_b} \sqrt{V(q) - V(q_f)}\, dq\right], \quad (13)$$

where v_0 is defined by the asymptotic form of the bounce trajectory $q(t)$ [4]: $q(\tau) \sim q_f + (v_0/|\lambda_-|)\exp[-|\lambda_-\tau|]$. Universal scaling laws can be derived close to criticality from (6), (7), and (8). The exponential factor in (13) follows the same scaling as $\sqrt{|\mathcal{E} - \mathcal{E}_-|}\, dq$. It therefore vanishes as $\sqrt{\delta^{3/2}}\,\delta^{1/2} = \delta^{5/4}$. From the asymptotic form of $q(t)$, dq follows the same law as $v_0/|\lambda_-|$. Thus $v_0 \sim \delta^{3/4}$ and the prefactor vanish as $\sqrt{\delta^{1/4}}\,\delta^{3/4} = \delta^{7/8}$. Note that these universal scaling laws agree with those already derived in the Gaussian case in [3].

The TIC (12) and MQT (13) decay rates obtained for the exact and Gaussian stationary states are shown in Fig. 3. To validate these results we checked that the Gaussian TIC decay rates computed in [8] are found when we (incorrectly at a finite distance from criticality) replace λ_+ by λ_- in Eq. (12) (data not shown). We also checked that our Gaussian MQT decay rate agrees with the one previously computed in [3].

The ICO atomic decay rates are also shown in Fig. 3. They are evaluated using the formula $d\mathcal{N}/dt = f_C(\mathcal{N})$ with $f_C(\mathcal{N}) = K\int|\psi|^4 d^3\tilde{\mathbf{x}} + L\int|\psi|^6 d^3\tilde{\mathbf{x}}$, where $K = 3.8 \times 10^{-4}\ \mathrm{s}^{-1}$ and $L = 2.6 \times 10^{-7}\ \mathrm{s}^{-1}$. Note that the ICO rate can be evaluated from the stable branch alone as done in [5,6]. In order to compare the particle decay rate $f_C(\mathcal{N})$ to the condensate collective decay rates obtained for TIC and MQT, we compute the condensate ICO half-life as $\tau_{1/2}(\mathcal{N}) = \int_{\mathcal{N}/2}^{\mathcal{N}} dn/f_C(n)$ and plot $\tau_{1/2}^{-1}$ in Fig. 3.

It is apparent by inspection of Fig. 3 that for a given value of $\mathcal{N}$ the exact and Gaussian approximate rates are dramatically different. We now compare the relative importance of the different exact decay rates. At $T \leq 1$ nK the MQT effect becomes important compared to the ICO decay in a region very close to $\mathcal{N}_c^E$ ($\delta \leq 8 \times 10^{-3}$) as it

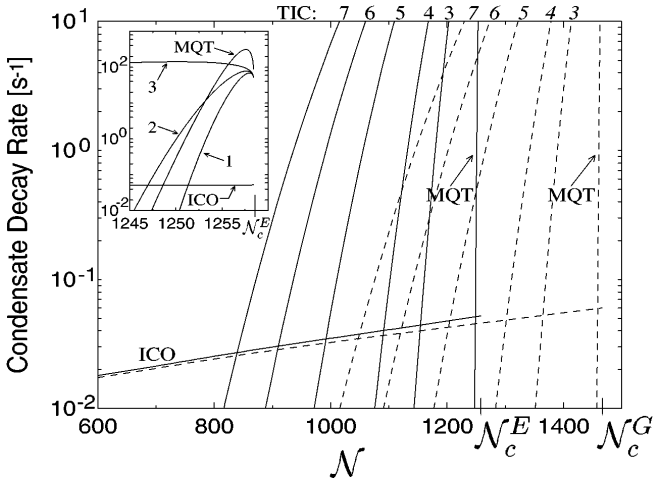

FIG. 3. Condensate decay rates versus particle number. ICO: inelastic collisions. MQT: macroscopic quantum tunneling. TIC: thermally induced collapse at temperatures 1 nK (1), 2 nK (2), 50 nK (3), 100 nK (4), 200 nK (5), 300 nK (6), and 400 nK (7). The inset shows the details of the crossover region between quantum tunneling and thermal decay rate. Solid lines: exact solution of the GP equation. Dashed lines: Gaussian approximation.

was shown in [3] using Gaussian computations but evaluating them with the exact maximal number of condensed particles $\mathcal{N}_c^E$. Considering thermal fluctuations for temperatures as low as 2 nK, it is apparent in Fig. 3 (see inset) that the MQT will be the dominant decay mechanism only in a region extremely close to $\mathcal{N}_c$ ($\delta < 5 \times 10^{-3}$) where the condensates will live less than 10^{-1} s. Thus, in the experimental case of ^{7}Li atoms, the relevant effects are ICO and TIC, with crossover determined in Fig. 3.

In summary, we found both the elliptic and hyperbolic exact stationary solutions of the GP equation, showing the presence of a generic HSN bifurcation. The Gaussian amplitudes for bifurcation scaling laws were found to be in substantial ($\geq$14%) error. The decay rates for the processes of MQT, ICO, and TIC were computed from the exact GP solutions. They were shown to obey universal scaling laws. Experimentally significant quantitative differences were found between the exact and Gaussian approximate rates. Future experimental determinations of decay processes should thus be compared to the present GP based rates.

[1] C. C. Bradley, C. A. Sackett, J. J. Tollett, and R. G. Hulet, Phys. Rev. Lett. **75**, 1687 (1995).
[2] C. C. Bradley, C. A. Sackett, and R. G. Hulet, Phys. Rev. Lett. **78**, 985 (1997).
[3] M. Ueda and A. J. Leggett, Phys. Rev. Lett. **80**, 1576 (1998).
[4] H. T. C. Stoof, J. Stat. Phys. **87**, 1353 (1997).
[5] H. Shi and W. Zheng, Phys. Rev. A **55**, 2930 (1997).
[6] R. J. Dodd *et al.*, Phys. Rev. A **54**, 661 (1996).
[7] Yu. Kagan, A. E. Muryshev, and G. V. Shlyapnikov, Phys. Rev. Lett. **81**, 933 (1998).
[8] C. A. Sackett, H. T. C. Stoof, and R. G. Hulet, Phys. Rev. Lett. **80**, 2031 (1998).
[9] P. A. Ruprecht, M. J. Holland, K. Burnett, and M. Edwards, Phys. Rev. A **51**, 4704 (1995).
[10] S. Inouye *et al.*, Nature (London) **392**, 151 (1998).
[11] E. P. Gross, Nuovo Cimento **20**, 454 (1961).
[12] L. P. Pitaevskii, Sov. Phys. JETP **13**, 451 (1961).
[13] M. Houbiers and H. T. C. Stoof, Phys. Rev. A **54**, 5055 (1996).
[14] D. Gottlieb and S. A. Orszag, *Numerical Analysis of Spectral Methods* (SIAM, Philadelphia, 1977).
[15] R. Seydel, *From Equilibrium to Chaos: Practical Bifurcation and Stability Analysis* (Elsevier, New York, 1988).
[16] C. Huepe, S. Métens, and M. E. Brachet (unpublished).
[17] C. Huepe and M. E. Brachet, C. R. Acad. Sci. Paris **325**, 195 (1997).
[18] C. Mamun and L. Tuckerman, Phys. Fluids **7**, 80 (1995).
[19] J. Guckenheimer and P. Holmes, *Nonlinear Oscillations, Dynamical Systems and Bifurcations of Vector Fields* (Springer-Verlag, Berlin, 1983).
[20] G. Baym and C. J. Pethick, Phys. Rev. Lett. **76**, 6 (1996).
[21] V. M. Pérez-Garća *et al.*, Phys. Rev. A **56**, 1424 (1997).
[22] C. Gardiner, *Handbook of Stochastic Methods* (Springer-Verlag, Berlin, 1985).